Third International Conference on Sustainable Construction Materials and Technologies http://www.claisse.info/Proceedings.htm

Self-healing of cracks by using saturated calcium hydroxide solution to activate slag in slag cementitious materials

Haoliang Huang[1]*, Guang Ye[1]

[1]*Microlab, Faculty of Civil Engineering and Geosciences, Delft university of Technology*
[*]*P.O. Box 5048 2600 GA DELFT, the Netherlands; haoliang.huang@tudelft.nl; g.ye@tudelft.nl*

ABSTRACT

It is well known that slag can be activated by alkali. However, using the activation of slag to trigger self-healing is still not clear. In this paper, self-healing of cracks by using saturated calcium hydroxide solution to active slag was investigated. The healing products formed in cracks were characterized by Fourier transform infrared spectroscopy (FTIR), thermogravimetric analysis (TGA) and environmental energy dispersive spectroscopy (ESEM) equipped with an energy dispersive spectroscopy (EDS). The efficiency of self-healing was evaluated by air permeability and ultra pulse velocity. The experimental result shows that the healing products formed within cracks are mainly C-S-H, ettringite and monocarboaluminate. The efficiency of self-healing as a function of time was evaluated by air permeability and ultra pulse velocity.

Keywords. self-healing, slag cement, calcium hydroxide solution

INTRODUCTION

Slag, as an industrial by-product, can be used to replace Portland cement and thereby the CO_2-emissions related to cement manufacturing can be reduced (Gartner, 2004, Juenger et al., 2010). This replacement can be beneficial to the sustainability of building construction to some extent. However, like Portland cement concrete, slag cement concrete is also a brittle composite material and cracks often occur when this material withstands tensile stress. These cracks facilitate the ingression of aggressive agents, such as chloride and sulphate, into concrete and reduce the durability of the concrete structures. Seeking ways to solve this problem has attracted lots of attention in recent years. Among the various techniques, self-healing is a potential solution. From the literature review, it can be known that when additional water accesses into cracks, further hydration of unhydrated cement or slag can make the cracks healed to some extent (Jacobsen et al., 1995, Jacobsen and Sellevold, 1996, Schlangen, 2006, van Tittelboom, 2012). Moreover, when both water and dissolved CO_3^{2-} are available, cracks can be healed by the crystallized $CaCO_3$ (Edvardsen, 1999, Granger et al., 2007). Based on this mechanism, bacterial which can accelerate the formation of $CaCO_3$ is used to promote self-healing of cracks (Jonkers et al., 2010). Apart from these, adhesive agents, such as cyanoacrylate (Dry, 2000), methyl methacrylate (Dry and McMillan, 1996) and polymeric agents (van Tittelboom, 2012), are also applied to seal cracks. Besides the aforementioned methods of self-healing, it may be also possible to trigger self-healing by activation of unhydrated slag with alkali solution in slag cementitious materials. However, the physicochemical process of self-healing triggered by the alkali-activation of slag is not understood completely and the corresponding self-healing efficiency is still obscure.

The aim of this study is to better understand the mechanism of self-healing triggered by alkali-activation of unhydrated slag, and also to evaluate the self-healing efficiency. To activate slag, several kinds of solutions such as Na_2SiO_3, NaOH can be used (Wang and Scrivener, 1995). However, the extra Na^+ ion may cause negative effects on concrete, for instance, alkali silica (aggregate) reaction. In comparison, $Ca(OH)_2$ solution is more compatible with concrete, since Ca is a main element in the matrix. Therefore, in this study saturated $Ca(OH)_2$ solution was used to activate the unhydrated slag for self-healing. In the experimental program, the healing products formed in cracks were characterized to explore the mineralogy by energy dispersive spectroscopy (EDS), Fourier transform infrared spectroscopy (FTIR) and thermogravimetric analysis/differential Thermal Analysis (TGA/DTG). In addition, the potential of self-healing triggered by the activation of slag was evaluated by air permeability tests (APT) and ultrasonic pulse velocity (UPV) measurements.

MATERIALS AND EXPERIMENTS

Materials and specimens. The materials used in this study were slag cement paste which was prepared with CEM III/B 42.5R. The water to cement ratio (w/c) was 0.3. As shown in Table 1, there were three series of specimens prepared for different tests in this research. The detailed information about the specimens is described as below.

Since it is difficult to obtain the healing products from real cracks for the characterization, planar gaps (Series I) were made to simulate the self-healing process, from which it is much easier to get the healing products. As shown in Figure 1(a), slices of cement paste at the age of 28 days were pressed together and cured in saturated $Ca(OH)_2$ solution for self-healing. After being healed for 14 days, slices of cement paste were separated and healing products were scratched off from the slice surfaces by a plastic sheet. Because the slices of cement paste were ground, the gap width is about 10 μm.

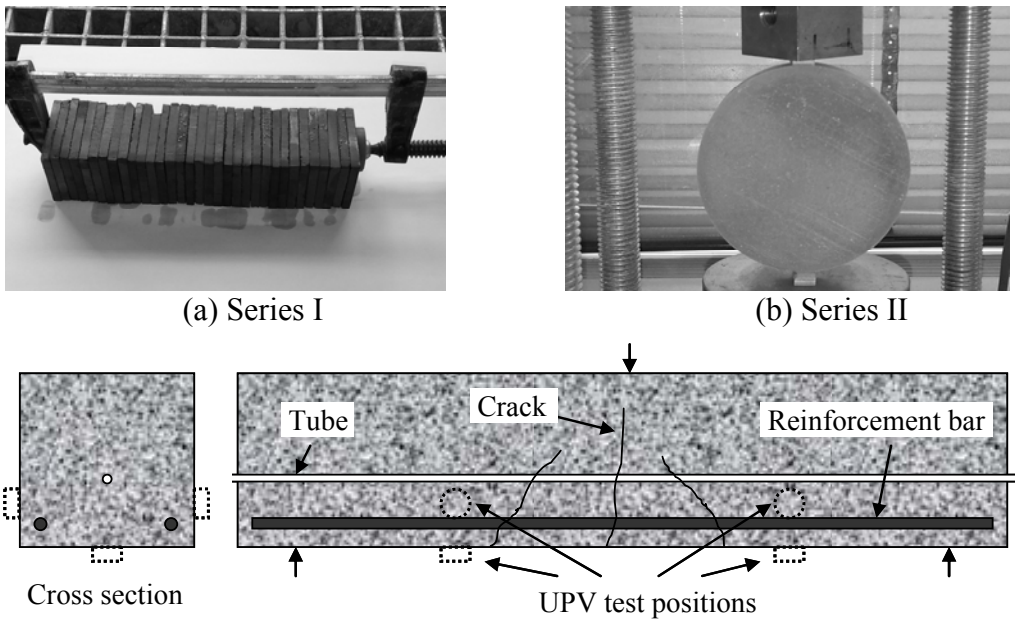

Figure 1. Different series of specimens

Table 1. Details about the materials and the specimens

Series	Materials						Specimens		Tests
	CEM III/B	w/c	QS	SF	SP	PVA fibers	Shape	Dimension (mm)	
I	1	0.3	-	-	-	-	Slice	40×40×5	EDS, FTIR, TGA
II	1	0.3	-	-	0.7%	1%	Cylinder	Φ100×15	Permeability
III	1	0.3	1.75	1%	1.5%	-	Prism	125×125×1000	UPV

Note: QS is quartz river sand 0/4 (by weight of cement); SF is silica fume (by weight of cement); SP is superplasticizer (by weight of cement).

In addition, cylinder specimens (Series II), with the diameter of 100 mm and thickness of 15 mm were casted for air permeability tests. In order to prevent the brittle collapse during the pre-cracking, 1% (by weight of cement) of PVA fibers was added into the specimens. As shown in Figure 1(b), the cylinder specimens at the age of 28 days were cracked by splitting and the ones with cracks of 10 ±3 μm were used for the air permeability tests (See Section 2.2.2).

Besides, specimens Series III were cast for ultrasonic pulse velocity measurement. As shown in Figure 1(c), a glass tube was embedded in the reinforced concrete beam with the dimensions of 125 mm × 125 mm × 1000 mm during the casting. The outside diameter of the glass tubes is 5 mm and the wall thickness is 1 mm. After being demoulded in the second day of casting, the specimens were cured for another 27 days in an air-conditioned room where the temperature is 20˚C ± 1˚C and the relative humidity is 99%. At the age of 28 days, the beams were cracked by three-point bending and the crack width is about 0.8 mm to 1 mm.

EXPERIMENTAL TECHNIQUES

EDS, FTIR and TGA/DTG. In order to explore the mechanism of self-healing by the activation of slag, EDS, FTIR and TGA/DTG were used to characterize the healing products. The chemical elements of healing products formed on the slice surfaces were tested by EDS. In addition, FTIR measurements were performed to determine the mineralogy of the healing products. The measures were conducted in transmission model in which the scan resolution is 4 cm^{-1} and there are 20 scans averaged for each measurement. Moreover, in order to get more specifics about the mineralogy of the healing products, TGA/DTG tests were performed in argon atmosphere at 1.5 bars. The heating rate was 10°C/min and the final temperature is 1100°C.

Air permeability tests. To evaluate the efficiency of self-healing, air permeability tests were carried out in this study. According to the literature, the relative pressure ($P_i - P_{atm}$) applied to the cracked sample ranged between 0.01 and 0.1 MPa (Picandet et al., 2001, Picandet et al., 2009). For this range of pressure, specific pressure regulators were used and the inlet air pressure was read by using a digital pressure gauge with an accuracy of 100 Pa. The outlet air percolating through the specimen was measured in atmospheric pressure using a soap bubble volumetric gas flow meter. The measurements were carried out in an air-conditioned room with the temperature of (20 ± 1 °C) and 50% relative humidity.

Each permeability test consists of a minimum of three measurements with different inlet pressures. Before reading, the air flow through the specimen should reach steady state. This

condition was verified by taking two measurements at a 10-minute interval. If the two readings differed by less than 2%, the steady state flow condition was assumed (Picandet et al., 2009). Prior to the tests, the specimens were dried by vacuating for 2 hours to guarantee that there is no water inside the cracks.

For each differential pressure, the apparent coefficient of permeability k_A (m^2) was calculated from the Hagen–Poiseuille relationship (Kollek, 1989):

$$k_i = \frac{2P_{atm}Q_iL\mu}{A(P_i^2 - P_{atm}^2)} \quad (1)$$

where L is the thickness of the sample (m), A is the cross-sectional area (m^2), Q_i is the measured gas flow (m^3/s), μ is the coefficient of viscosity, P_i is the inlet pressure (Pa), and P_{atm} is the atmospheric pressure (Pa).

By means of the air permeability tests, the efficiency of self-healing induced by both saturated $Ca(OH)_2$ solution and additional water was evaluated. In this paper, the efficiency of self-healing was defined as:

$$e = (1 - \frac{k(t)}{k_0}) \times 100\% \quad (2)$$

where $k(t)$ is air permeability after self-healing at time t, k_0 is the original air permeability before self-healing.

Ultrasonic pulse velocity measurements. In order to evaluate the self-healing efficiency, ultrasonic pulse velocity measurements were conducted as well. When the medium is isotropic, the wavelength is large compared to the size of inhomogeneities and the velocity of longitudinal waves c_L is:

$$c_L = \sqrt{\frac{E(1-\nu)}{\rho(1+\nu)(1-2\nu)}} \quad (3)$$

where E is Young's modulus, ν is Poisson's Ratio and ρ is density of the medium. Since liquids or gaps can not support shear stresses, Equation (3) can be rewritten as:

$$c_L = \sqrt{\frac{K}{\rho}} \quad (4)$$

where K is the bulk modulus.

According to Equation (3) and (4), the transmission of ultrasonic pulse through the air is much slower than that through the solid. The ultrasonic pulse velocity through the concrete specimens remarkably decreases after the concrete specimens crack. On the other hand, after the cracked specimens are healed, the ultrasonic pulse velocity rises up again due to the solid healing products formed in cracks. In this research, the initial ultrasonic pulse velocity was measured before the 28-days-old specimens were cracked. After that, the specimens were cracked by three-point bending until the width of crack ranged between 0.8 mm to 1 mm. The ultrasonic pulse velocity was measured again after the cracking. In this study, saturated $Ca(OH)_2$ solution for self-healing was injected into 3 specimens through the embedded glass tubes, while another 3 specimens as reference were cured without injected solution . After that, the ultrasonic pulse velocity of the specimens was measured to follow the self-healing of cracks at 20, 45, 80, 200 and 300 hours.

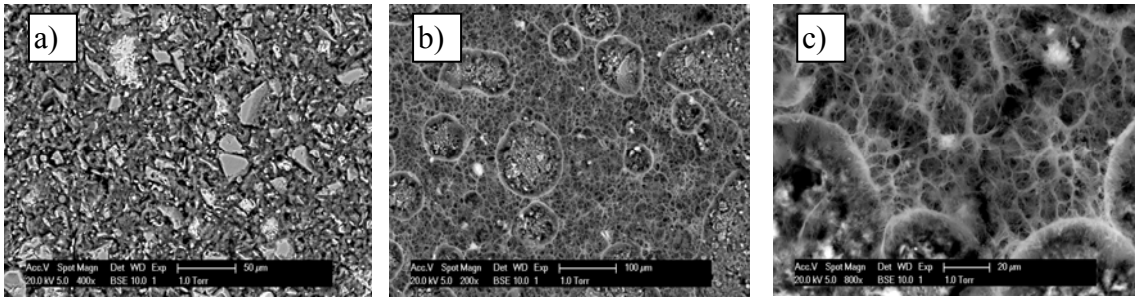

Figure 2. Morphology of the slice surface: (a) before self-healing, (b) after self-healing (magnification: 200X) and (c) after self-healing (magnification: 800X)

RESULTS AND DISCUSSION

Morphology and EDS analysis. Figure 2(a) shows the morphology of the slice surfaces at the age of 28 days before self-healing, while Figure 2 (b) and (c) displays the morphology of the slice surfaces after being heal for 250 hours. It can be seen that due to the polish in preparation procedures, the surfaces of slices are flat and different solid phases in the matrix can be distinguished before self-healing. After self-healing, there are some gel-like healing products formed on the slice surfaces and these healing products make the slice surfaces obviously different from those before self-healing.

The chemical elements of the healing products on the slice surfaces were analyzed by EDS. In this research, random positions at healing products on 3 slice surfaces were tested. As shown in Figure 3, Ca/Si ratio ranges from 0.9 to 1.7 with a mean value of 1.2, which is similar to that of the hydration products in matrix. With respect to Al/Si, it fluctuates between 0.15 and 0.35, of which the mean value is 0.21. In addition, the mean Mg/Si is 0.23, which is similar to Al/Si. From the EDS results, it is found that the main chemical elements of the healing products are Ca, Si, Al and Mg. However, only with this information, the mineralogy of the healing products still can not be determined. Further investigation was carried out by using FTIR and TGA/DTG.

FTIR. Figure 4 shows the FTIR results of CEM III/B, CEMIII/B paste and healing products scratched from the slice surfaces. All these samples have a complex group of bands in the range between 800 cm^{-1} and 1200 cm^{-1}, corresponding to the stretching vibration of Si-O bonds (Yu et al., 1999) and asymmetric stretching of SO_4^{2-} in sulphate phase (Barnett et al., 2002, Myneni et al., 1998). In addition, the bands in the range of 1400-1500 cm^{-1} correspond to the asymmetric stretching of CO_3^{2-} (Yu et al., 1999), caused by the incorporation of CO_2 when the sample is exposed in air. The bands between 1640 to 1650 cm^{-1} is due to H-O-H bending vibration of molecular H_2O (Yu et al., 1999). The broad band in the range of 2800-3700 cm^{-1} corresponds to stretching vibrations of O-H groups in H_2O or hydroxyls with a wide range of hydrogen-bond strengths (Yu et al., 1999).

As the hydration of CEM III/B takes place, the main band at 877 cm^{-1} in the profile of CEMIII/B shifts to 955 cm^{-1} in the profile of CEMIII/B paste, corresponding to the Si-O stretching vibrations in C-S-H gels (Ghosh and Handoo, 1980, Yu et al., 1999). Moreover, the shoulder at 1099 cm^{-1} in the profile of CEMIII/B paste is attributed to SO_4^{2-} in sulphate phase (Barnett et al., 2002, Myneni et al., 1998). Additionally, both in the profiles of CEMIII/B paste and healing products, the bands in the range of 1400-1500 cm^{-1} corresponding to CO_3^{2-} can be contributed by calcium carbonate and hydrotalcite. Because of

H_2O in hydrated CEMIII/B paste, bands at 1640-1650 cm^{-1} and 2800-3700 cm^{-1} occurs in the profile of CEMIII/B paste. By comparing the profile of healing products to the one of CEMIII/B paste, it is interesting to note that the positions of main bands in the profile of healing products are almost the same as the CEMIII/B paste. What should be mentioned is that the band at 1099 cm^{-1} in the profile of healing products is much more obvious than that in the profile of CEMIII/B paste. It indicates more sulphate phase in healing products.

TGA/DTG. In addition to FTIR test, the healing products are also characterized by TGA/DTG. From Figure 5, it can be seen that the sample weight of slag cement paste decreases significantly when the temperature increases from 40˚C to 200˚C. Correspondingly, there is an apparent peak at 130˚C in the DTG profile of slag cement paste. In addition, a small peak occurs at 480˚C and 700˚C in this DTG profile. With respect to the healing products, the weight lost of the sample is much larger than that of bulk paste. There is a remarkable peak observed in the corresponding DTG profile at 150˚C. Moreover, there are small shoulders at 180˚C and 285˚C. When the temperature increases to 480˚C, a small peak occurs. Another two peaks appears at 760˚C and 830˚C respectively.

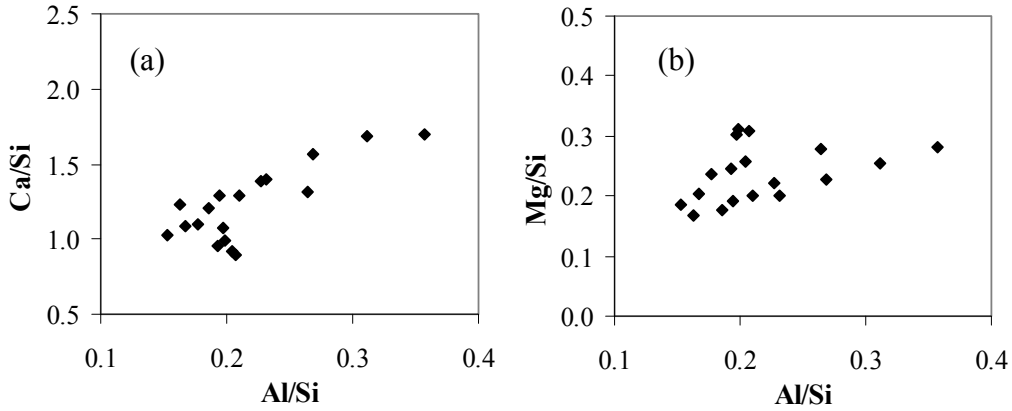

Figure 3. Atomic ratios of healing products

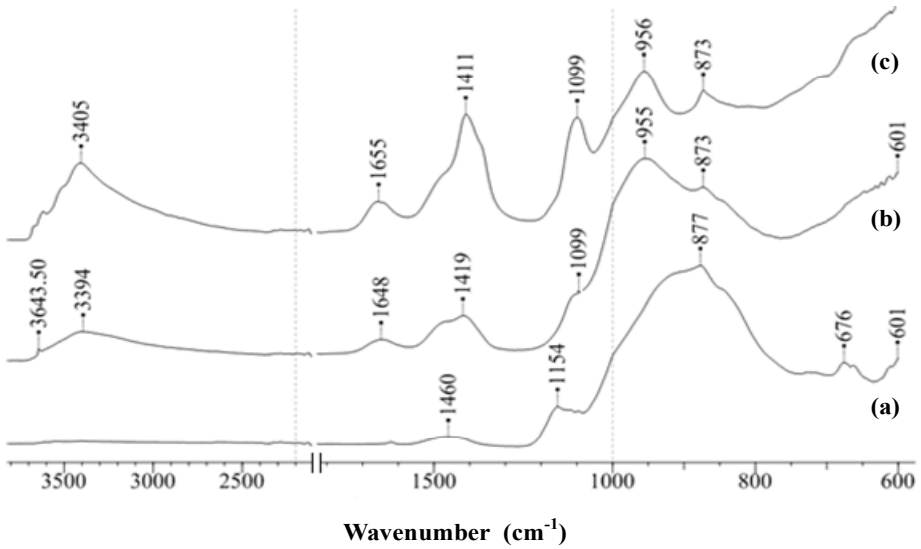

Figure 4. FTIR results: (a) CEM III/B, (b) CEMIII/B paste and (c) healing products

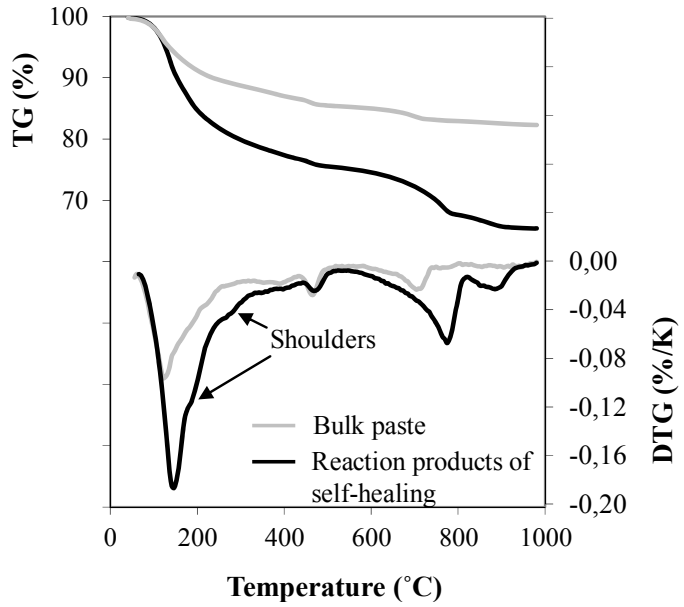

Figure 5. TG/DTG results of reaction products of self-healing and bulk paste

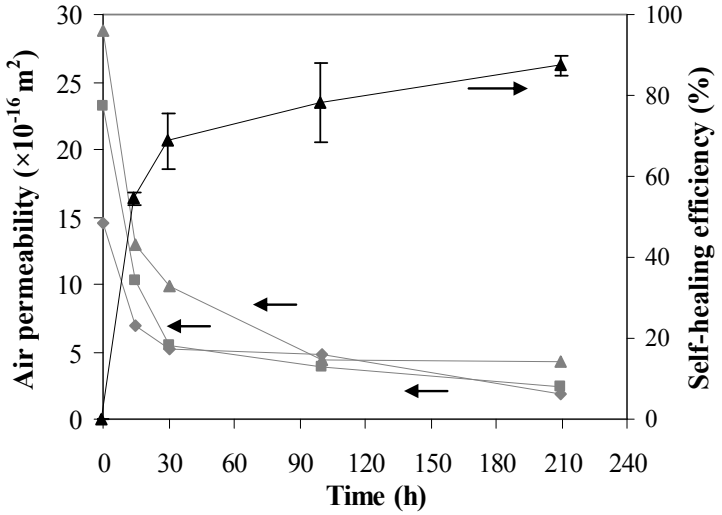

Figure 6. Air permeability of slag cement paste as a function of self-healing time

From the literature (Haha et al., 2011), it can be learned that the peak in DTG profile before 200˚C indicates the decomposition of ettringite and CSH. Moreover, according to Chowaniec (Chowaniec, 2012), the decomposition of monocarboaluminate mainly takes place at about 160˚C, 280˚C, 680˚C, 800˚C and 860˚C. Therefore, the DTG profile for the healing products in this study indicates the presence of monocarboaluminate. In addition, $CaCO_3$ usually decomposes between 630˚C and 860˚C (Halikia et al., 2001). Therefore, the decomposition of $CaCO_3$ can also contribute the weight loss between 630˚C and 860˚C. Apart from these, the small peak at 480 °C both in the DTG profiles for reaction products and bulk paste can be caused by the decomposition of portlandite. In CEMIII/B paste, there should be no portlandite because of the large percentage of slag which consumes portlandite during the hydration. Therefore, the detected portlandite in the reaction products of self-healing can be contributed by the

saturated $Ca(OH)_2$ solution used as the healing agent. Although the healing process was under sealed conditions, after the samples were taken out of saturated $Ca(OH)_2$ solution, they were exposed to the atmosphere. This exposure can lead to the carbonation of portlandite. As a result, calcite was presented in the reaction products of self-healing. However, the portlandite and calcite can not be considered as the reaction products of self-healing. Based on this analysis, it could conclude that the main minerals in the reaction products of self-healing in slag cement paste are C-S-H, ettringite and monocarboaluminate.

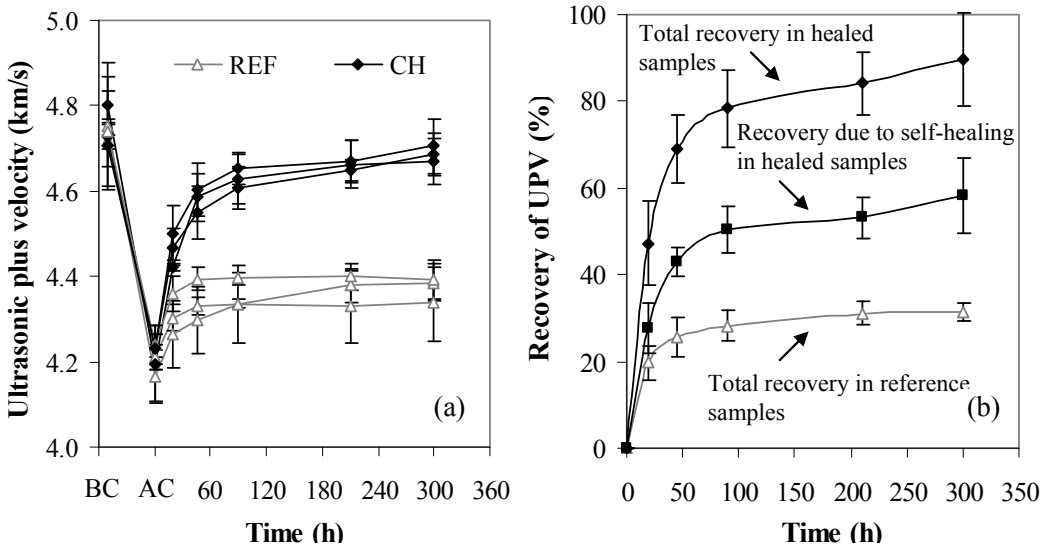

Figure 7. Evaluation of self-healing by ultrasonic pulse velocity: (a) ultrasonic pulse velocity at different stages (BC refers to "before cracking" and AC refers to "after cracking"); (b) recovery of ultrasonic pulse velocity.

Air permeability tests. Air permeability of the specimens after self-healing by saturated $Ca(OH)_2$ solution is shown in Figure 6. From the results, it can be found that the air permeability decreases dramatically after being healed for 30 hours. After 30 hours, the decrease of air permeability becomes slower and slower. Correspondingly, the efficiency of self-healing reaches about 70% after being healed by saturated $Ca(OH)_2$ solution for 30 hours.

Ultrasonic pulse velocity tests. Figure 7(a) shows the ultrasonic pulse velocity of the specimens at different stages: before cracking, after cracking and after healing. From this figure, it can be seen that the ultrasonic pulse velocity decreases sharply after the specimens crack. The reason is that the transmission of ultrasonic pulse through the air in cracks is much slower than that through the concrete. As being cured for a certain time after cracking, the ultrasonic pulse velocity increases gradually. As shown in Figure 7(b), when the reference specimens (without solution for self-healing) were cured for 45 hours after cracking, the ultrasonic pulse velocity recovers by about 25%. After that, the recovery develops much slower and only several percentage of recovery is obtained from 45 hours to 300 hours. In comparison, for the specimen with CH solution the recovery of ultrasonic pulse velocity grows much faster both during the first 45 hours and the later period. As known, due to the rebound of the reinforced bars, the width of cracks reduces gradually after cracking. This causes the main recovery of ultrasonic pulse velocity through the reference specimens during the first 45 hours after cracking. According to the literature (Ye et al., 2001), as the hydration of cement going on, the cement paste becomes denser and denser.

This also results in the increase of ultrasonic pulse velocity through the reference specimens during the later period (after 45 hours).

For the specimens healed by saturated $Ca(OH)_2$ solution, the recovery of ultrasonic pulse velocity is not only attributed to the rebound of reinforce bars and the ongoing hydration, but also the self-healing of cracks triggered by the solution. In order to evaluate the self-healing of cracks, the recovery of ultrasonic pulse velocity caused by the rebound of reinforce bars and the ongoing hydration is eliminated from the total recovery in the specimens healed by saturated $Ca(OH)_2$ solution. In this way, the recovery of ultrasonic pulse velocity due to self-healing of cracks can be determined. As shown in Figure 7(b), the recovery of ultrasonic pulse velocity through the healed specimens is mainly contributed by self-healing. Consistent with the air permeability results, the results of UPV tests also show that the progress of self-healing mainly takes place before 50 hours.

CONCLUSIONS

In this paper, the mechanism and efficiency of self-healing by using saturated $Ca(OH)_2$ solution to activate slag in slag cementitious materials were investigated by FTIR, TGA/DTG, air permeability test and ultrasonic pulse velocity measurements. Based on experimental results, conclusions can be drawn as follow:

- The healing products formed in cracks are mainly C-S-H, ettringite and monocarboaluminate while using saturated $Ca(OH)_2$ solution to activate the unreacted slag for self-healing.
- From air permeability and ultrasonic pulse velocity tests, it can be learned that self-healing of cracks takes place fast in the first 50 hours and after that, the progress of self-healing starts to slow down.
- Self-healing of cracks in slag cementitious materials can be triggered by using saturated $Ca(OH)_2$ solution to activate unreacted slag.

ACKNOWLEDGEMENTS

The authors would like to thank the China Scholarship Council (CSC) for the financial support for this work.

REFERENCES

Barnett, S.J., Macphee, D.E., Lachowski, E.E., and Crammond, N.J., (2002). "Xrd, edx and ir analysis of solid solutions between thaumasite and ettringite." *Cement and Concrete Research*, 32(5):719-730.

Chowaniec, O., (2012). *"Limestone addition in cement."* Thesis (PhD). ÉCOLE POLYTECHNIQUE FÉDÉRALE DE LAUSANNE.

Dry, C. and McMillan, W., (1996). "Three-part methylmethacrylate adhesive system as an internal delivery system for smart responsive concrete." *Smart Mater Struct*, 5(3):297-300.

Dry, C.M., (2000). "Three designs for the internal release of sealants, adhesives, and waterproofing chemicals into concrete to reduce permeability." *Cement and Concrete Research*, 30(12):1969-1977.

Edvardsen, C., (1999). "Water permeability and autogenous healing of cracks in concrete." *ACI Materials Journal*, 96(4):448-454.

Gartner, E., (2004). "Industrially interesting approaches to low-co2 cements." *Cement and*

Concrete Research, 34(9):1489-1498.
Ghosh, S.N. and Handoo, S.K., (1980). "Infrared and raman spectral studies in cement and concrete (review)." *Cement and Concrete Research*, 10(6):771-782.
Granger, S., Loukili, A., Pijaudier-Cabot, G., and Chanvillard, G., (2007). "Experimental characterization of the self-healing of cracks in an ultra high performance cementitious material: Mechanical tests and acoustic emission analysis." *Cement and Concrete Research*, 37(4):519-527.
Haha, M.B., Lothenbach, B., Le Saout, G., and Winnefeld, F., (2011). "Influence of slag chemistry on the hydration of alkali-activated blast-furnace slag â€" part ii: Effect of al2o3." *Cement and Concrete Research*, 42(1):74-83.
Halikia, I., Zoumpoulakis, L., Christodoulou, E., and Prattis, D., (2001). "Kinetic study of the thermal decomposition of calcium carbonate by isothermal methods of analysis." *The European Journal of Mineral Processing and Environmental Protection*, 1(2):89-102.
Jacobsen, S., Marchand, J., and Hornain, H., (1995). "Sem observations of the microstructure of frost deteriorated and self-healed concretes." *Cement and Concrete Research*, 25(8):1781-1790.
Jacobsen, S. and Sellevold, E.J., (1996). "Self healing of high strength concrete after deterioration by freeze/thaw." *Cement and Concrete Research*, 26(1):55-62.
Jonkers, H.M., Thijssen, A., Muyzer, G., Copuroglu, O., and Schlangen, E., (2010). "Application of bacteria as self-healing agent for the development of sustainable concrete." *Ecological Engineering*, 36(2):230-235.
Juenger, M.C.G., Winnefeld, F., Provis, J.L., and Ideker, J.H., (2010). "Advances in alternative cementitious binders." *Cement and Concrete Research*, 41(12):1232-1243.
Kollek, J., (1989). "The determination of the permeability of concrete to oxygen by the cembureau method—a recommendation." *Materials and Structures*, 22(3):225-230.
Myneni, S.C.B., Traina, S.J., Waychunas, G.A., and Logan, T.J., (1998). "Vibrational spectroscopy of functional group chemistry and arsenate coordination in ettringite." *Geochimica et Cosmochimica Acta*, 62(21–22):3499-3514.
Picandet, V., Khelidj, A., and Bastian, G., (2001). "Effect of axial compressive damage on gas permeability of ordinary and high-performance concrete." *Cement and Concrete Research*, 31(11):1525-1532.
Picandet, V., Khelidj, A., and Bellegou, H., (2009). "Crack effects on gas and water permeability of concretes." *Cement and Concrete Research*, 39(6):537-547.
Schlangen, E., ter Heide, N. and van Breugel, K., (2006). "Crack healing of early age cracks in concrete." In: M.S. Konsta-Gdoutos, Eds. *Measuring, monitoring and modeling concrete properties*. Netherlands: Springer.
van Tittelboom, K., (2012). *"Self-healing concrete through incorporation of encapsulated bacteria- or polymer-based healing agents."* Thesis (doctor). Ghent University.
Wang, S.-D. and Scrivener, K.L., (1995). "Hydration products of alkali activated slag cement." *Cement and Concrete Research*, 25(3):561-571.
Ye, G., Van Breugel, K., and Fraaij, A., (2001). "Experimental study on ultrasonic pulse velocity evaluation of the microstructure of cementitious material at early age." *Heron*, 46(3):161-167.
Yu, P., Kirkpatrick, R.J., Poe, B., McMillan, P.F., and Cong, X., (1999). "Structure of calcium silicate hydrate (c-s-h): Near-, mid-, and far-infrared spectroscopy." *Journal of the American Ceramic Society*, 82(3):742-748.